A LARGE SCALE DUAL-POROSITY APPROACH FOR THE MODELING OF WORMHOLING PHENOMENON

C. E. COHEN[1], D. DING[1], M. QUINTARD[2] AND B. BAZIN[1]

[1] *Institut Français du Pétrole, 1 & 4 avenue de Bois-Préau, 92852 Rueil Malmaison, France*

[2] *Institut de Mécanique des Fluides de Toulouse, allée Camille Soula, 31400 Toulouse, France*

ABSTRACT

Acid treatment is frequently used in the oil industry to improve well productivity. It is achieved in carbonate reservoir by taking advantage of a macroscopic instability which creates empty channels (wormholes) bypassing the damaged areas and improving near wellbore permeability. Length, size and density of these channels depend on numerous parameters from injection rate to rock properties. Significant efforts have been made in both experimental and numerical studies in order to optimise stimulation procedures. Today, core-scale numerical models can successfully reproduce the dissolution physical mechanism, but they are limited in their ability to simulate wormhole at the wellbore scale. Therefore, large-scale models are based on semi-empirical approaches.

In this paper, we first present a preliminary analysis of core-scale simulations. We have studied the effect of confinement on core scale experiments and simulations. In the second part we introduce a large scale model obtained through upscaling techniques from the core-scale model. In the large scale model, the dual-porosity concept is used to take into account the different physical processes occurring in the wormholes and matrix areas. Acid transport and rock dissolution equations are written in each medium, and a transfer term is introduced to describe fluid exchange between these two media. Examples show that the dual-porosity model can be used to describe carbonate acidizing at large scale. This model can reproduce different types of dissolution pattern, from compact to uniform through wormholing regimes.

To determine physical parameters in the large scale dual-porosity model, an inversion procedure is used to match experimental data or data from core-scale model simulations. An objective function is built to optimize pressure drop and porosity variation, at different time and space steps. This approach is illustrated by examples. The developed large-scale dual-porosity model will be used for 3D near-wellbore simulations to evaluate skin factors along acidified well sections. In this way, we will be able to design an optimum acid stimulation procedure for field applications.

1. INTRODUCTION

Acid injection is commonly used in the oil industry to improve, or at least recover, well productivity. This technique increases near-well permeability, therefore improving production flow rate. This treatment is applied in particular for cases of formation damage, after drilling or long uninterrupted production. In case of a carbonated reservoir, the aim of acid stimulation is to create empty channels called wormholes. In successful stimulation jobs, wormholes bypass the damaged area near wellbore, and become a pathway for the oil

reservoir to reach the well. This technique has poorly evolved during the last forty years. But today, as the drilling of horizontal wells, which may consume large quantities of acid, has become widely spread in the industry, there is a growing interest for understanding dissolution mechanisms. The interaction between acid transport, chemical reaction, and heterogeneities encountered at different scales, defines the unstable behaviour of wormholing and so, the success of the treatment.

Dissolution can be described through the different length scales involved in the process. At the pore scale, the reaction kinetic at the pore surface, and the transport of acid and reaction products to the surface, control the dissolution. If the reaction characteristic time at the pore surface is smaller than the characteristic time of mass transport thought the pore boundary layer, the dissolution is called mass-transfer-limited. In the other case, when the kinetic of the surface reaction is very slow compared to the transport of acid at the pore surface, it is called reaction-rate-limited. These dissolution mechanisms lead to different core-scale descriptions, depending on the rate at which acid is consumed when the fluid enters into the porous medium. Local equilibrium dissolution, i.e., rapid acid consumption, leads to very sharp fronts, whereas non-equilibrium dissolution is characterized by fronts with porosity variations over a significant distance. A link between pore-scale and core-scale is that reaction-rate-limited dissolution produces for lower flow rate local non-equilibrium dissolution than mass-transfer limited dissolution. Higher scale is the section-scale or well-scale, where wormholes compete against each other for flow rate and produce complex dissolution pattern. At this scale, it is necessary to consider wormhole density but also formation heterogeneities which have a great influence on the dissolution pattern. We can calculate at this scale an equivalent permeability tensor for an elementary volume containing several wormholes. The final length scale is the reservoir scale where the effect of an acid stimulation is measured through a single parameter called skin, which express the bound between the well and the reservoir.

Several methods such as network modelling (Daccord *et al*, 1989),(Fredd *et al*, 1998),(Hoefner *et al*, 1988), stochastic models (Daccord, 1987),(Pichler *et al*, 1992) or capillary tube (Buisje, 1997),(Fredd *et al*, 1999),(Huang *et al*, 1999),(Wang *et al*, 1993) have been used to study all those mechanisms. Golfier *et al* (Golfier, 2001),(Golfier *et al*, 2002), have developed, using the method of volume averaging, a general non-equilibrium dissolution model that has been applied successfully to simulate core-scale dissolution problems. This model can reproduce most dissolution patterns observed at the core scale. We first present in this paper some simulations using the model of Golfier, which give us an insight on how the dimensions of the core can affect wormholing and optimal injection conditions. We also investigate the evolution of wormhole versus flow rate changes. Unfortunately this model is unable to realise simulation at the section scale because of today computation resources limitations. For this reason, we present in the second part a large scale model based on a dual porosity concept which can be used to simulate full-scale acid treatment. To build this model, we apply first the volume averaging method to the core scale equations. We consider for this matter two volumes, one containing dominant growing wormholes, and the other short lived wormholes and compact dissolution. A transfer term between the two volumes reproduce the flow rate derivation in favour of dominant wormholes. A fractional flow function is introduced in the convection term to reproduce macroscopic dispersion of the wormhole volume fraction. Finally, we discuss the introduction of two different models of the dissolution term. In this dual-porosity model, large scale parameters are determined through

an inversion procedure. This model is designed to reproduce all kind of dissolution figures, from compact dissolution through ramified wormholes.

2. CORE-SCALE SIMULATION

The basic equations for core-scale simulation were described by Golfier (Golfier, 2001),(Golfier *et al*, 2002). Based on these equations, we simulate wormholes dissolution processes in an unconfined domain and investigate radial flow dissolution.

2.1 Effect of domain confinement on wormholes growth. A domain is called "confined" when the length of the dominant wormhole at breakthrough, is much longer than the characteristic length of the injection area. Most experimental studies or simulations using local non-equilibrium models or network models, were achieved in confined conditions. To express this effect of domain geometry, we define a shape factor F. For 2D domains, F is the ratio of the height over the length. Unconfined domains or domains of great extension have a shape factor F greater than unity. FIGURE 1a shows the evolution of the dominant wormhole length over time, for different value of F, and illustrates the impact of confinement on wormhole growth.

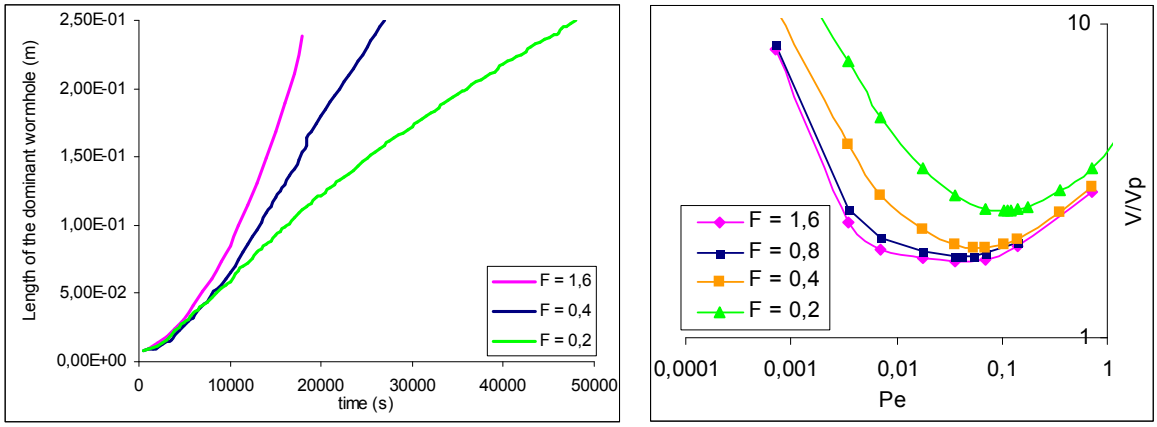

(a) (b)

FIGURE 1. (a) Length of the dominant wormhole over time. (b) Volume of acid for breakthrough, normalized by pores volume, as a function of the Péclet number.

In a confined case (F = 0.2), the wormhole competition duration is very short, and gives birth to a unique dominant wormhole which attracts almost all the flow rate available. So the entering flow rate in this dominant wormhole become constant because limited by the total flow rate entering the sample. The growth of the dominant wormhole is then only driven by diffusion and fluid loss. Those two mechanisms slow down wormhole growth and their influence increase with the length of the wormhole. Consequently, the growth rate of the dominant wormhole decrease with time. In the unconfined case (F = 1.4), wormholes are still competing for flow rate until breakthrough occurs, and the dominant wormhole see its entering flow rate increasing all along the dissolution process. This leads to an increase of the dominant wormhole growth rate with time. The major consequence is that breakthrough occurs much earlier in unconfined cases as illustrated in FIGURE 1b.

FIGURE 1b shows the volume of acid necessary for breakthrough, normalized by pores volume, in function of the Péclet number, for different values of F. As explained by Hung (Hung *et al*, 1987), diffusion stimulate wormhole competition and accelerate the selection of a unique dominant wormhole. For this reason, the difference of behaviour between confined and unconfined samples increases as the Péclet number decreases, as long as the dissolution regime produce wormholes. The main consequence of those results is that the optimum injection rate is lower for a unconfined case than for a confined case. This means that optimum conditions for acid stimulations revealed by experiments on core samples *may not be valid on the field*.

This observations on the confinement effect were made on linear flow, but we also realised radial flow simulations (FIGURE 2).

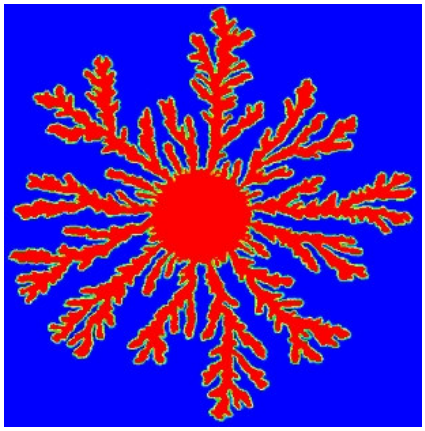

FIGURE 2. Core-scale simulation of radial flow

Our preliminary results in this configuration seem to show that radius of the well versus the size of the domain play a similar role as F in the linear case. Small well radius or large domain will accelerate the selection of dominant wormholes.

3. SECTION-SCALE MODELLING

We present in this section a section-scale model to simulate complete acid treatments, based on a extension of the preliminary dual-porosity dissolution model proposed by Golfier (Golfier, 2001).

3.1 Presentation of the section-scale model. The proposed model is first obtained from a volume averaging of the core-scale model. FIGURE 3 illustrates our dual-porosity approach, in which the porous medium is divided into two volumes. One volume contains all the dominant growing wormholes (V_H), and the other contains all the short lived wormholes and compact dissolution (V_M).

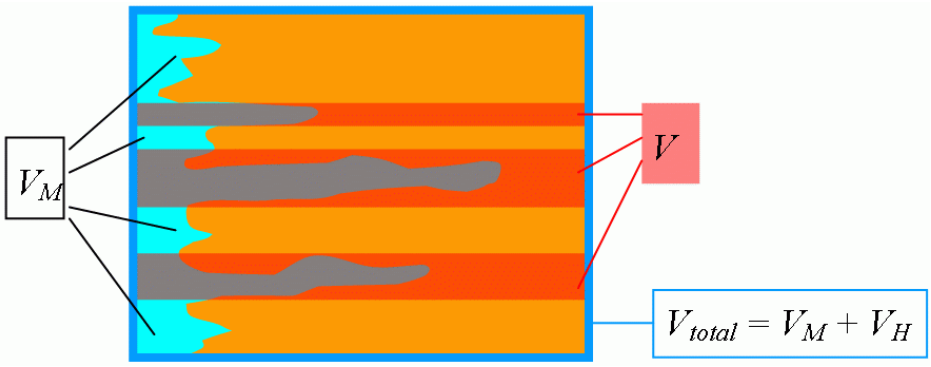

FIGURE 3. Dual-porosity description of an acid stimulated porous medium at the section-scale

The dual-porosity approach is commonly used to describe media with large contrasts of properties. For example, dual-porosity models are used for fractured porous media. Our problem has the specificity that the contrast of properties between the two media starts from small perturbations and will increase with dissolution. The length expected for a dominant wormhole in a successful acid stimulation is only a few meters. It gives us the opportunity to work in a limited bandwidth of wormholes length, and to consider the ratio between the two volumes constant in space and time.

For each medium, our section-scale model is made of a transport equation for the acid species, a flow equation, a mass balance equation for the fluid phase, and a mass balance equation for the solid phase. The volume fraction of the two media are noted ϕ_M and ϕ_H, with $\phi_M + \phi_H = 1$. The variables of pressure, concentration, velocity and porosity in the section-scale are expressed in our model as

$$P_H^* = \langle P_\beta \rangle_H^H = \frac{1}{V_H} \int_{V_H} P_\beta dV \quad ; \quad P_M^* = \langle P_\beta \rangle_M^M = \frac{1}{V_M} \int_{V_M} P_\beta dV \tag{1}$$

$$C_H^* = \langle C_{A\beta} \rangle_H^H = \frac{1}{V_H} \int_{V_H} C_{A\beta} dV \quad ; \quad C_M^* = \langle C_{A\beta} \rangle_M^M = \frac{1}{V_M} \int_{V_M} C_{A\beta} dV \tag{2}$$

$$\mathrm{V}_H^* = \langle \mathrm{V}_\beta \rangle_H^H = \frac{1}{V_H} \int_{V_H} \mathrm{V}_\beta dV \quad ; \quad \mathrm{V}_M^* = \langle \mathrm{V}_\beta \rangle_M^M = \frac{1}{V_M} \int_{V_M} \mathrm{V}_\beta dV \tag{3}$$

$$\varepsilon_H^* = \langle \varepsilon_\beta \rangle_H^H = \frac{1}{V_H} \int_{V_H} \varepsilon_\beta dV \quad ; \quad \varepsilon_M^* = \langle \varepsilon_\beta \rangle_M^M = \frac{1}{V_M} \int_{V_M} \varepsilon_\beta dV \tag{4}$$

where P_β, $C_{A\beta}$, V_β and ε_β are the expression of the pressure, concentration, superficial velocity and porosity at the core-scale. The mass balance equation for the fluid phase is given by :

$$\nabla.\left(\phi_M \mathrm{V}_M^*\right) + \psi^* \left(P_M^* - P_H^*\right) = 0 \tag{5}$$

$$\nabla.\left(\phi_H \mathrm{V}_H^*\right) - \psi^* \left(P_M^* - P_H^*\right) = 0 \tag{6}$$

where ψ^* is the coefficient for the transfer term between these two media. V^*_H and V^*_M are calculated using Darcy's law :

$$V^*_M = -\frac{K^*_M}{\mu}.\nabla P^*_M \tag{7}$$

$$V^*_H = -\frac{K^*_H}{\mu}.\nabla P^*_H \tag{8}$$

with K^*_H and K^*_M permeability tensors. The coefficient ψ^* is calculated by assuming a periodical spatial arrangement of dominant wormholes. Our description of the transfer term link the coefficient ψ^* to a parameter which is a characteristic length. The mass balance equation for the solid phase is given by :

$$\frac{\partial \varepsilon^*_H}{\partial t} = N_{ac} g^*_H \tag{9}$$

$$\frac{\partial \varepsilon^*_M}{\partial t} = N_{ac} g^*_M \tag{10}$$

where N_{ac} is the acid capacity number, g_H^* and g_M^* are two functions modelling the averaged dissolution term. Those functions also appear in the acid transport equations

$$\phi_H \varepsilon^*_H \frac{\partial C^*_H}{\partial t} + \nabla.\left(\phi_H V^*_H f^H\right) - \psi^* C_{H-M}\left(P^*_M - P^*_H\right) = -\phi_H g^*_H \tag{11}$$

$$\phi_M \varepsilon^*_M \frac{\partial C^*_M}{\partial t} + \nabla.\left(\phi_M V^*_M f^M\right) + \psi^* C_{H-M}\left(P^*_M - P^*_H\right) = -\phi_M g^*_M \tag{12}$$

where we introduced the fractional flow functions f^H and f^M (Lenormand, 1996) to model dispersion in each medium. For the dissolution terms g_H^* and g_M^* , we tried two different expressions. The first ones are written g_{1H}^* and g_{1M}^* , and are inspired by the dissolution term given by Golfier at the core-scale (Golfier, 2001)

$$g^*_{1H} = C^*_H A\left(1-\varepsilon^*_H\right)^{2/3} \tag{13}$$

$$g^*_{1M} = C^*_M A\left(1-\varepsilon^*_M\right)^{2/3} \tag{14}$$

But this expression has the inconvenience of producing dissolution in all elementary volumes which contain both acid and rock, when in fact dissolution is only significant when tips are passing by elementary volume. For this reason we proposed other forms of the dissolution terms (g_{1H}^* and g_{1M}*), linked to the local flux balance of acid, i.e., the convection term :

$$g_{2M}^{*} = \frac{\alpha_M}{\phi_M} \nabla . \left(\phi_M \mathrm{V}_M^{*} f^{M} \right) \tag{15}$$

$$g_{2H}^{*} = \frac{\alpha_H}{\phi_H} \nabla . \left(\phi_H \mathrm{V}_H^{*} f^{H} \right) \tag{16}$$

The whole system is closed with a simple permeability-porosity relation depending on one parameter. To determine the parameters in our model, we used core-scale simulations to provide reference data, and we applied an inversion procedure using the Levenberg-Marquart algorithm. For the inversion procedure, an objective function is built through the comparison of porosity fields and pressure drop inside the domain. This method can also use experimental results as reference data.

3.2 Results and comparison. Our model has been tested for different types of dissolution, from compact dissolution to ramified wormholes. Core-scale simulations are considered as reference solutions. Comparisons are made from core-scale and section-scale simulations. The example in FIGURE 4 illustrates the comparison for both dissolution terms, at a constant injection velocity, in the case of conical wormholes.

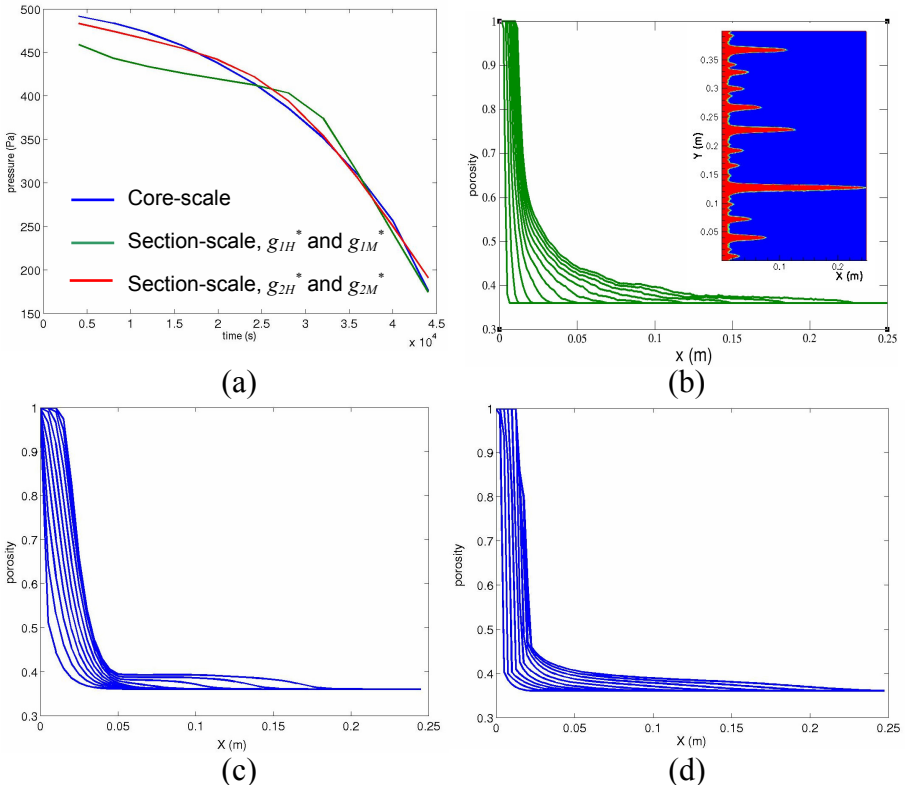

FIGURE 4. Comparison between core-scale simulation and section-scale simulations for an injection velocity of 4,64.10-6 m.s-1. (a) pressure drop in the sample versus time. (b), (c), and (d) are porosity from at different time step. (b) core-scale simulation. (c) section-scale simulation using g_{1H}^{*} and g_{1M}^{*}. (d) section-scale simulation using g_{2H}^{*} and g_{2M}^{*}.

Simulations show that our section-scale model using dissolution term g_{1H}^* and g_{1M}^* can reproduce fairly well the dissolution process for compact dissolution and dominant wormhole dissolution. For conical wormholes, the competition between wormholes is very intense and the transition between the two length scales (short lived wormholes and dominant wormholes) is very smooth. In this case, the model using dissolution term g_{1H}^* and g_{1M}^* produces a more brutal transition, with a pressure drop which does not properly match core-scale results. We observe a similar behaviour with the ramified wormholes.

When using the dissolution terms g_{2H}^* and g_{2M}^*, section-scale simulations show good agreement for all kind of dissolution patterns, even for conical (FIGURE 4) and ramified wormholes. In general, this model gives us satisfactory results and creates the possibility to study entire acid treatments at reservoir scale.

4. CONCLUSION

This work provides further understanding and modelling of acid stimulations at both core-scale and section-scale. Core-scale simulations show that the size of the domain can highly influence the dissolution process, making results from laboratory experiments inappropriate for field application. A dual-porosity model is presented for the simulation of acid dissolution at the section-scale. This will give us the opportunity to simulate complete acid treatment, and therefore, to optimise design of acid stimulations.

REFERENCES

Buisje, M. A. (1997), Understanding Wormholing Mechanisms Can Improve Acid Treatments in Carbonate Formations. SPE 38166, SPE European Formation Damage Conference.

Daccord G. (1987), Chemical Dissolution of a Porous Media by a Reactive I, Physical Review Letters, Vol. 58, pp. 479-482.

Daccord, G., E. Touboul and R. Lenormand (1989), Carbonate Acidizing: Toward a Quantitative Model of the Wormholing Phenomenon. SPE 16887,

Fredd, C. N. and H. S. Fogler (1998), Alternative Stimulation Fluids and Their Impact on Carbonate Acidizing, *SPE Journal*, SPE 31074.

Fredd, C. N. and H. S. Fogler (1999), Optimum Conditions for Wormhole Formation in Carbonate Porous Media: Influence of Transport and Reaction, *SPE Journal*, SPE 50337.

Golfier F., (2001), Dissolution des Roches Carbonatées après par l'Injection d'Acide, Ph.D. Thesis, Institut National Polytechnique de Toulouse.

Golfier, F., C. Zarcone, B. Bazin, R. Lenormand, D. Lasseux and M. Quintard (2002), On The Ability of a Darcy-Scale Model to Capure Wormhole Formation During the Dissolution of a Porous Media, *Journal of Fluid Mechanics*, Vol. 547, n° pp. 213-254.

Hoefner, M. L. and H. s. Fogler (1988), Pore Evolution and Channel Formation During Flow and Reaction in Porous Media, *AIChE*, Vol. 34, n° 1, pp. 45-54.

Huang, T., D. Zhu and A. D. Hill (1999), Prediction of Wormhole Population Density in Carbonate Matrix Acidizing. SPE54723, European Formation Damage Conference.

Hung, K. M. and A. D. Hill (1987), A Mechanistic Model of Wormhole Growth in Carbonate Matrix Acidizing and Fracturing. SPE 16886, 62nd Annual Technical conference and Exhibition.

Lenormand, R., (1996), Transport Equations for Fluid Displacements in Stratified Porous Media: The MHD Model, *SPE Journal*, SPE 30797.

Pichler , T., T. P. Frick and M. J. Economides (1992), Stochastic Modeling of Wormhole Growth in Carbonate Acidizing. SPE 25004, European Petroleum Conference.

Wang, Y., A. D. Hill and R. S. Schechter (1993), The Optimum Injection Rate for Matrix Acidizing of Carbonate. SPE 26579, 68th Annual Technical Conference and Exhibition.